

# Investigating the influence of fabrication parameters, flax-fibre reinforcement and ageing on interlaminar shear strength in thermoplastic-bonded wood veneers

Clément Prunier<sup>1,2</sup>, Jérôme Rousseau<sup>1</sup>, Pauline Butaud<sup>2</sup>, Thomas Jeannin<sup>2</sup>, Xavier Gabrion<sup>2</sup>, Vincent Placet<sup>2</sup>

1 : Laboratoire DRIVE  
Université de Bourgogne, Nevers, France  
clement.prunier@u-bourgogne.fr, jerome.rousseau@u-bourgogne.fr

2 : Université de Franche-Comté  
SUPMICROTECH-ENSMM, CNRS, Institut FEMTO-ST, F-25000 Besançon, France  
pauline.butaud@univ-fcomte.fr, thomas.jeannin@femto-st.fr, xavier.gabrion@femto-st.fr, vincent.placet@univ-fcomte.fr

## Abstract

This study investigates the suitability of two thermoplastic polymers that are non-toxic and environmentally friendly, namely polylactic acid (PLA) and recycled maleic anhydride grafted polypropylene (rMAPP), as potential alternatives to formaldehyde-based adhesives in plywood production. Two types of rotary-cut wood veneers, beech and Douglas fir, are tested. The performance of interfaces is evaluated using interlaminar shear strength tests, and compared to those obtained with a benchmark polyvinyl glue. This study examines the manufacturing process settings on interlaminar shear strength, as well as the influence of incorporating plant fibre reinforcement into the adhesive. It also evaluates the effects of accelerated ageing on the shear strength. The results indicate that manufacturing parameters tested within the specified range have a limited impact on shear strength. Both rMAPP and polyvinyl glue exhibit similar performance. This strong adhesion obtained with rMAPP is attributed to the formation of covalent bonds between the maleic anhydride (MA) and the hydroxyl groups within the amorphous constituents of the wood cell wall, and to mechanical interlocking resulting from the polymer's efficient penetration into the various wood pore structures, including cell lumens and lathe checks. The incorporation of flax fibres enhances interface performance under ambient conditions but has a negative effect in the case of hygro- and hydro-thermal accelerated ageing. The results with PLA adhesive show more varied outcomes, with lower shear strength when manufactured via vacuum bagging technique. Furthermore, the performance of PLA adhesive does not meet plywood ageing standards due to its moisture sensitivity and susceptibility to hydrolysis degradation.

## Keywords

Plywood, bonding, natural fibres, ageing, adhesive, hybrid materials

## 1. Introduction

For the last twenty years, the use of renewable materials in industry has gained relevance due to various environmental concerns facing our society. In the plywood industry, the most frequently used adhesives are urea-formaldehyde (UF), melamine-urea-formaldehyde (MUF) and phenol-urea-formaldehyde (PUF). These thermoset adhesives are petroleum-based and have a significant environmental footprint both during their production process and at the end of their lifecycle. Additionally, they present some health hazards [1]. Substituting these adhesives with environmentally friendly alternatives is the subject of extensive research [2].

The use of bio-sourced resins, primarily derived from tannins and lignin, is well documented in the literature and shows promising outcomes. In some cases, mechanical performance is comparable to that of traditional adhesives, despite having certain limitations in terms of humidity resistance [3–8]. The use of thermoplastic resins as adhesives for plywood is also an interesting alternative due to their recyclability advantages. Bekhta et al. [9] tested the adhesion quality of birch and beech plywood bonded with low density polyethylene (LDPE), co-polyamid (CoPA) and co-polyester (CoPE). They observed adhesion properties approaching those of industrial glues and even exceeding them for CoPA. Other studies have shown that the use of recycled polypropylene (rPP) as an adhesive for plywood results in higher interlaminar shear strength (ILSS) compared to traditional formaldehyde-based adhesives [10, 11]. Gaugler et al. [12] investigated high-density polyethylene (HDPE), thermoplastic polyurethane (TPU) and polylactic acid (PLA) in amorphous and semi-crystalline phases, to determine their suitability as adhesives for maple, beech and spruce veneers. Their study revealed the superiority of PLA over other adhesives, due to its higher polarity. Luedtke et al. [13] continued this study and showed that the quality of the bond was dependent on the parameters of the manufacturing process. The excellent performance of PLA as a plywood adhesive was subsequently corroborated by Grigsby et al. [14], who also demonstrated that amorphous PLA outperformed semi-crystalline PLA in achieving a stronger bondline in plywood.

Fibres can also be incorporated into the adhesive to produce advanced engineering materials with enhanced performance. Bal et al. [15] observed that the modulus of elasticity and ultimate stress increased when reinforcing poplar plywoods with glass fibre fabrics. Studies showed that these types of reinforcements have an impact on the ILSS value, which is influenced by factors such as adhesive type [16] and fibre orientation [17]. Fibres with lower environmental impact such as basalt fibre [18], bamboo fibre [19, 20] have also displayed promising performance as interface reinforcements. However, Jorda et al. [21] observed no significant effect of flax and cellulose fibre reinforcements on beech plywoods,

raising questions about reinforcement dependency on fibre areal weight, and adhesive choice. Despite their many environmental benefits, plant fibres are also characterized by a high sensitivity to moisture, especially when compared to the traditional synthetic fibres such as glass and carbon. That is why it is important to evaluate the humidity and immersion resistance of new adhesives reinforced with such fibres as it provides insights into their ageing behaviour and suitability for specific applications. Bio-based adhesives can also be sensitive to moisture, which warrants a thorough evaluation of their durability.

Literature points out that plywoods bonded with PLA exhibit minimal degradation of their ILSS when immersed in cold water [14], meeting ASTM/HPVA industrial criteria [22]. However, degradations have been observed when plywoods are immersed in water at temperatures above 60 °C due to the degradation of PLA ester groups [23]. Kajaks et al. [10] observed that plywood glued with polypropylene showed a reduction in ILSS of approximately 60% when immersed in cold water for 24 h. However, the hydrophobic nature of polypropylene makes it resistant to accelerated ageing processes in hot and boiling water, meeting the standards for plywood adhesives [11]. Research has also demonstrated the possibility of improving humidity resistance and adhesion between polypropylene and lignocellulosic materials by grafting it with maleic anhydride (MA), which allows esterification between O-H groups and maleic anhydride molecules [11, 24, 25]. Studies of ageing over several days and in different atmospheric conditions show a dependence of the mechanical behaviour of plywood on relative humidity and temperature caused by swelling of the substrates, which varies with the type of adhesive [26, 27]. Long-term ageing of thermoplastic polymers when used as a matrix for plant fibre reinforced plastics (FRP) shows that the presence of fibres affects the overall ageing behaviour of the composite, with degradation occurring at the fibre / matrix interfaces [28] due to fibre swelling during water uptake [29]. One might observe that literature lacks information relating to interlaminar performances of plywoods made of low-quality veneers, as well as knowledge regarding ageing behaviour of interfaces made of recycled or bio-sourced thermoplastics and plant fibres.

So, this study proposes a comparative analysis of the adhesive bond strength between wood veneers using a traditional vinyl adhesive and adhesives with a reduced environmental impact, namely PLA and recycled PP grafted with maleic anhydride. These adhesives were selected to represent two distinct approaches for developing plywood adhesives with minimised carbon footprints and toxic emissions, in contrast to the conventional formaldehyde-based adhesives commonly used in the industry.

PP is a widely utilised polymer with a broad range of applications, ranging from high-end to commodity uses, including agricultural consumables, and represents 21% of the non-fibre plastic production since 1950 [30]. The recycled PP investigated in this study originates from such agricultural consumables. It also allows for a reduction in its environmental impact, as its pellets production have a Global Warming Potential (GWP) of 0.19 kg CO<sub>2</sub> eq./kg of polymer (for a ratio of 90% of recycled PP), against 1.86 kg

CO<sub>2</sub> eq./kg of polymer for virgin pellets. For comparison, urea-formaldehyde (UF) based adhesives have a global warming potential of 5.00kg CO<sub>2</sub> eq./kg of resin, and 3.66 kg CO<sub>2</sub> eq./kg of resin for phenol-formaldehyde (PF) based adhesives. GWP values are issued from the EcoInvent3 database. PP production volume was of 79 million tons in 2018 [31].

The inherent hydrophobic nature of PP presents challenges when forming strong bonds with hydrophilic materials like wood. However, this limitation can be overcome by grafting it with a compatibiliser, such as maleic anhydride. As mentioned before, this process enables the creation of covalent bonds between the PP molecules and the hydroxyl groups available on natural fibres [25]. By replacing some of the hydroxyl groups on the wood polymers with organic anhydride, the hygroscopic properties of the wood are reduced [32].

On the other hand, PLA stands as a prime illustration of bio-based adhesives, derived from abundant biomass like maize [33], with no toxicity, and better environmental profile, as it has a global warming potential of 3.09 kg CO<sub>2</sub> eq./kg of polymer (values issued from EcoInvent3 database, excluding the biogenic carbon component). Its production volume, of 494 thousand tons in 2023, is estimated to reach around 2.9 million tons in 2028 [34].

Bio-based adhesives offer good properties such as their excellent compatibility with bio-based materials due to their hydrophilicity, good mechanical performance, and potential for biodegradation. However, their hydrophilic nature and propensity for biodegradation impose limitations on their potential application fields, warranting thorough examination.

This research also involves two different wood species: beech, a wood commonly used in the European plywood industry and serving as a reference material, and Douglas fir, a local wood type used to explore new applications, particularly for the lowest graded wood pieces. The investigation also delves into the effects on interface performance of plywood manufacturing parameters, ageing and the incorporation of flax fibres within the adhesive.

In this paper, the first section presents the materials studied, the samples fabrication process, the testing methods and the various post-processing studies carried out on the results. The second section is dedicated to the presentation and discussion of the findings pertaining to the influence of the fabrication parameters, flax UD reinforcement and ageing on ILSS and fracture behaviour. Lastly, the conclusions drawn from these studies are comprehensively reviewed in the final section.

## **2. Material and Method**

### *2.1. Materials*

The plywoods studied are made from either beech (*Fagus sylvatica*) or Douglas fir (*Pseudotsuga menziesii*) veneers from the Centre-Val de Loire and Bourgogne-Franche-Comté regions of France,

respectively. They are rotary cut and provided by the LaBoMaP (processes and materials laboratory), Cluny, France. The veneers are 2 mm thick for beech and 3 mm for Douglas fir. The Douglas fir veneers are thicker because they are more fragile, making them more difficult to cut with a lathe while maintaining a thinner thickness. They are considered as low-quality veneers because of the high number of cracks and knots. Their average density at 15% moisture content is 710 kg/m<sup>3</sup> for beech and 500 kg/m<sup>3</sup> for Douglas fir. After cutting, the veneers are dried, and then stored under non-controlled ambient relative humidity and temperature.

Three adhesives are studied. The first one is a polypropylene recycled from agricultural wastes, provided by the company Adivalor. It is mixed with 5 wt% of a polypropylene grafted with maleic anhydride (rMAPP) Polybond ® 3200, which contains 1 wt% of pure maleic anhydride (MA). It is extruded into 70 µm thick films using a calender extruder. Its melting flow index (MFI) is 6 g/10 min (measured at 230 °C, with a 2.16 kg load). Its ultimate tensile strain is 918% +/- 45%. The second adhesive, denoted as “PLE 005”, is a PLA resin supplied by Natureplast with a crystallinity index of 30% to 40%. It is processed through a calender extruder to produce 100 µm thick films. This adhesive has a melt flow index (MFI) of 10 g/10 min (measured at 190 °C with a 2.16 kg load). Its ultimate tensile strain is approximately 5%. The third adhesive used as a reference is a common polyvinyl based wood glue Paracol Wood D3®.

The reinforcement fibres used are in the form of unidirectional flax fibre tape (FlaxTape ®), supplied by Ecotechnilin, France. The tape has an areal weight of 110 g/m<sup>2</sup>. The fibres are stored at 23 °C and 50% RH for a minimum of 48 hours prior to manufacture.

## 2.2. *Fabrication*

The veneers are stacked in the sequence [0/90/0]. In this sequence, the 0° orientation is aligned with the longitudinal direction of the wood (L) and the x axis of the plate, whereas the 90° orientation is aligned with the tangential direction of the wood (T) and the y axis of the plate. This stratification (**Fig. 1(a)**) is chosen to ensure that the two middle veneers have the same orientation, which is a requirement for the standard test described in section 2.4. The orientation of veneers with respect to opened or closed sides, which depends on the presence of lathe checks, is randomly selected in this study and is therefore not one of the parameters studied. Two adhesive film sheets are placed between each veneer. For both adhesives, the temperature is set at 180 °C, as this provides good flowability for rMAPP and PLA while remaining below the degradation temperature of flax fibres [35] and wood [36].

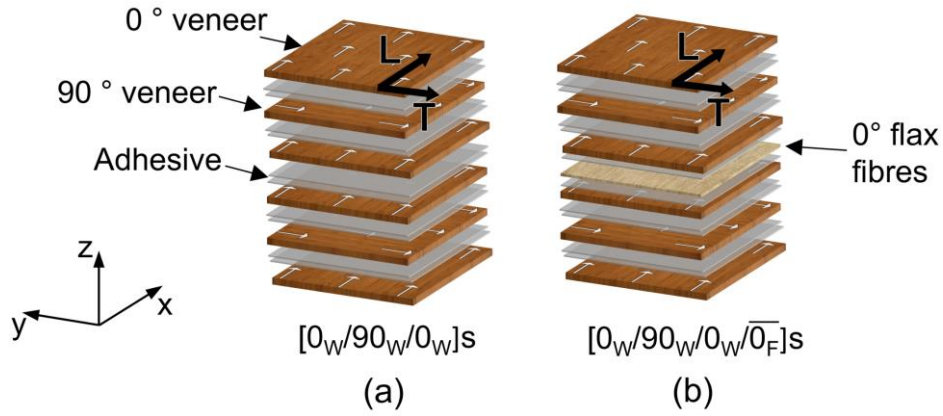


**Fig. 1** Schematic representation of plywood stratification, (a) without flax fibre reinforcement and (b) with flax fibre reinforcement. In the stratification nomenclature, W is for Wood veneer, and F is for Flax Fibre ply.

A Fontijne LaboPro 600 press is used for thermocompression. The manufacturing process is as follows. First, the stack is inserted in the press, and the thermocompression process begins. The press closes, and starts heating to the set temperature at a rate of 15 °C/min. Once the desired temperature is reached, the selected pressure is applied for a given period, which is divided into two segments. The first segment has a fixed duration dependent on the veneer species. It is the time needed to reach the target temperature in the core of the plywood. It is determined once for each configuration by monitoring temperature with a thermocouple positioned between the middle veneers of the plywood. The second segment is a variable time added to the fixed duration and referred to as Additional Heating Time (AHT). AHT is a parameter considered in the optimisation phase of this study. The platens are then cooled down at a rate of 20 °C/min until they reach ambient temperature. The press then releases pressure and opens. When investigating the effect of fibre reinforcement, a layer of unidirectional flax fibres is inserted between the two adhesive film sheets of the middle layer (**Fig. 1(b)**). **Fig.2** displays the temperature evolution within the plywood core, along with the set temperature and pressure applied.

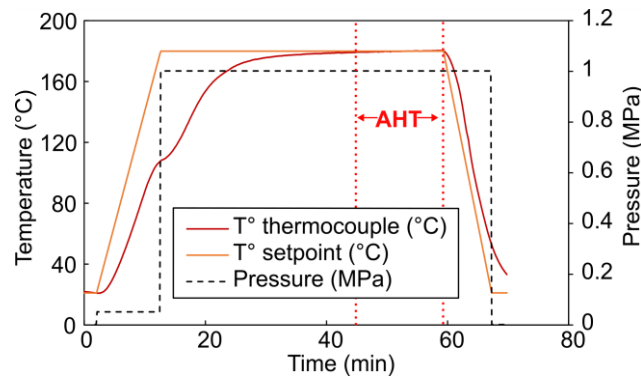


**Fig.2** Evolution of temperature and pressure between plywood's middle veneers during the fabrication process

For vacuum bagging, the plywood is heated in a Memmert® UF 450 oven. The fabrication process remains the same as for thermocompression, with two notable differences: a heating rate of 4.5 °C/min and cooling achieved by opening the oven doors.

Reference plates are produced by a cold press process using polyvinyl glue. The glue is applied to one side of the veneers with a roller at a rate of 150 to 200 g/m<sup>2</sup>. The veneers are then assembled under a press with a pressure of 6 bars for a minimum duration of 20 minutes.

The newly manufactured plywood is then stored at 50% RH and 23 °C for a minimum of 48 hours before being tested.

The parameters employed in the production of plywood without flax fibres, using both thermocompression and vacuum bagging techniques, are summarised in **Table 1**. Meanwhile, the parameters used in the manufacturing of plywood with flax fibres and for ageing tests are presented in **Table 2**.

**Table 1** Summary of fabrication parameters and composition of the tested plywoods

Wood	Adhesive Type and mass (g)	Fixed heating time (min)	Additional heating time – AHT (min)	Pressure (MPa)
Beech	rMAPP - 92 g; PLA – 181 g	34	5; 15	Vacuum (0.1); 1 and 2
Douglas fir	rMAPP - 92 g; PLA - 181 g	51	5; 15	Vacuum (0.1); 1 and 2

**Table 2** Summary of the fabrication parameters of the plates used for the fibre reinforcement and ageing studies

Sample	Wood	Adhesive Type	AHT (min)	Pressure (MPa)
Fibre reinforcement	Beech; Douglas fir	rMAPP PLA	5; 15	1
Ageing	Beech; Douglas fir	rMAPP PLA	15	

The produced plywood plates are cut into 7 samples (25 × 100 mm<sup>2</sup>) following EN 302 standard recommendations. Subsequently, notches are made on both sides of each sample, resulting in grooves 3 mm wide and 25 mm apart. These grooves reach a depth equivalent to three veneer layers. A schematic representation of the final sample shape is depicted in **Fig.3**. The area between the two grooves is referred to as the overlap area, measuring 25 × 25 mm<sup>2</sup>. When the specimen is subjected to tensile loading, the overlap surface is subjected to shear loading, allowing ILSS to be measured for different interface configurations.  $\mu\text{m}$

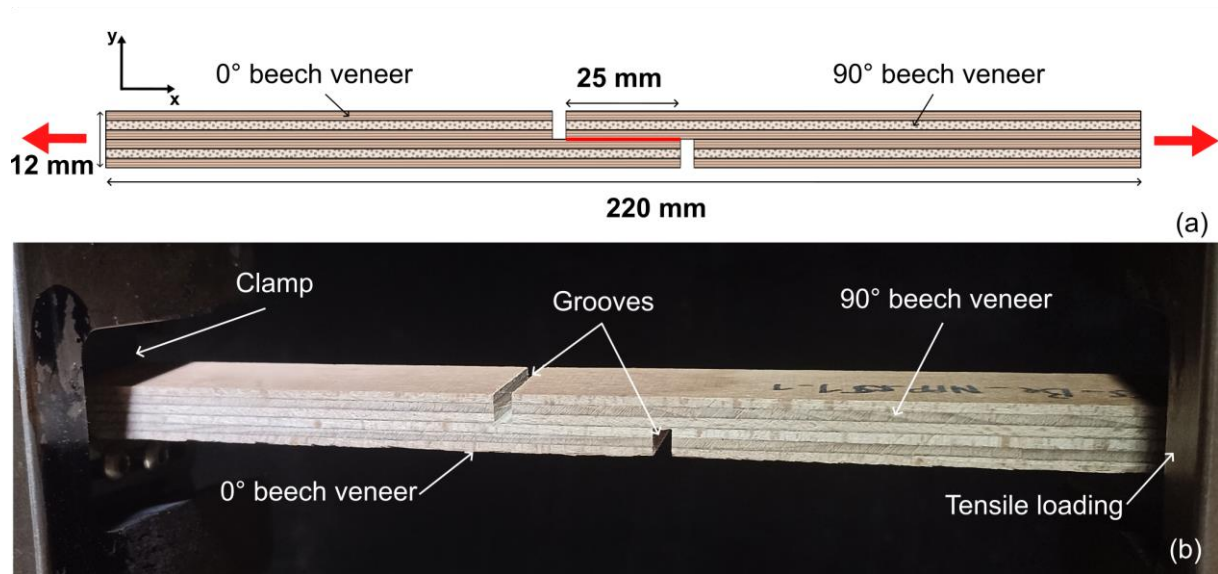


**Fig.3** Schematic representation of the test samples used for interlaminar shear strength measurement (a). Photo of an interlaminar shear strength test sample before testing (b).

### 2.3. Ageing methods

7 samples of each group of components listed in **Table 2** are subjected to accelerated ageing by two different methods, each with a different degree of severity. The first method, labelled “Ag1” (for Ageing 1), draws inspiration from the works of Scida et al. [37], who studied the hydrothermal ageing of flax/epoxy composites. In this method, the samples are aged in a Q-SUN-XE-3® climatic chamber with a relative humidity of 90% and a temperature of 40 °C for 40 days. Samples are then placed in a climatic chamber at the same hydrothermal conditions as those used for unaged samples conditioning (23 °C 50% RH), until stabilization of their relative humidity. The second method, designated “Ag2”, is derived from the EN 314 standard, which is used for testing the adhesion of plywood. It consists of immersing the samples in boiling water for 6 hours. Samples are then placed in a climatic chamber at 23 °C 50% RH until stabilization of their relative humidity. Its severe aspect allows for testing the limits of adhesives. These ageing methods are applied to samples with beech or Douglas fir veneers, bonded with either MAPP or PLA adhesive, and with or without flax fibres reinforcement.

### 2.4. Interlaminar shear strength (ILSS) tests

Interlaminar shear strength tests are conducted using a tensile testing machine MTS C45 equipped with a 100 kN load cell. The tests are carried out at a crosshead displacement speed of 2 mm/min. In **Fig.3(a)** the applied forces are indicated by red arrows, and the shear test area is highlighted in red. The direction of tensile testing coincides with the wood grain orientation (L-direction) in both the middle and outer



veneers. Throughout the test, the force and crosshead displacement are recorded over time. The ILSS is subsequently calculated by dividing the tensile strength by the overlap area.

The results are analysed using various statistical methods and tools.-The statistical methods used are detailed in the Online Resource 1.

### *2.5. Microscopic and X-Ray microtomography observations*

Microscopic observations are conducted to examine the configuration of the interface across various material compositions. Samples are cut transversely in a region outside the overlap area, polished, and observed using a Keyence VHX 6000 digital microscope.

Some samples are scanned by X-Ray Computed Tomography (CT) on an EasyTom machine from RX Solution, and the X-ray transmission images (projections) are acquired using a 2530DX detector of  $2176 \times 1792$  pixels<sup>2</sup>. All the details concerning the X-ray microtomography conditions and parameters are described in the Online Resource 2.

## **3. Results and discussions**

### *3.1. Influence of manufacturing parameters on interface behaviour*

#### **Interlaminar shear strength**

**Fig.4** presents the results obtained from ILSS tests conducted on beech plywood samples manufactured under the different combinations of pressure and heating times and with the three selected adhesives, vinylic glue (VG) as a reference, rMAPP, and PLA. Configurations are represented by a nomenclature that includes the adhesive used, the pressure value and the additional heating time. The results of statistical Tukey's and Dunn's tests are marked with letters next to the mean result, indicating whether or not the results are significantly different from each other. Mean value and standard deviations are represented with red dot and red lines. The box plots illustrate the median value, first (Q1) and third (Q3) quartiles, and extreme values (whiskers). Outliers are not included in the box plots. Results are summarised in **Appendix 1**. The overall findings indicate that both rMAPP and PLA yield ILSS values within the same range as the reference adhesive. The mean ILSS values ranges from 6.5 MPa to 8.3 MPa with rMAPP and from 5.7 MPa to 7.6 MPa with PLA adhesive, while the reference adhesive yields ILSS values from 6.4 MPa to 9.8 MPa. The ILSS results of rMAPP fall within the range observed by Kajaks et al. [38] for birch veneers bonded with MA grafted PP, with values ranging from 6.82 MPa to 12.62 MPa. ILSS values obtained with PLA closely align with those reported by Luedtke et al. [13] for beech veneers, ranging from 6.70 MPa to 9.56 MPa. As expected, results exhibit considerable variation. Testing wood materials inherently involves statistical aspects, influenced by material heterogeneities, defects and singularities. The coefficient of variation ranges from 2.8% to 29.7% depending on the

sample lots. Therefore, a statistical approach is clearly necessary to ensure a reliable comparison of the results. The Tukey’s post-hoc test indicated that most of the configurations yielded ILSS values within the same distribution, represented by the letter “b”, as the vinylic glue reference. The only configurations that are statistically different from the reference are the samples made with PLA under vacuum conditions, whose distribution is represented by the letter “a”. The beech-PLA samples manufactured under vacuum with a 5-minute AHT are not depicted in the figure because the veneer samples delaminated immediately after the manufacturing. Vacuum bagging demonstrated overall poor performance for beech plywoods glued with PLA adhesive. Based on these findings, it is not recommended to use vacuum bagging for this particular combination of materials and adhesive.

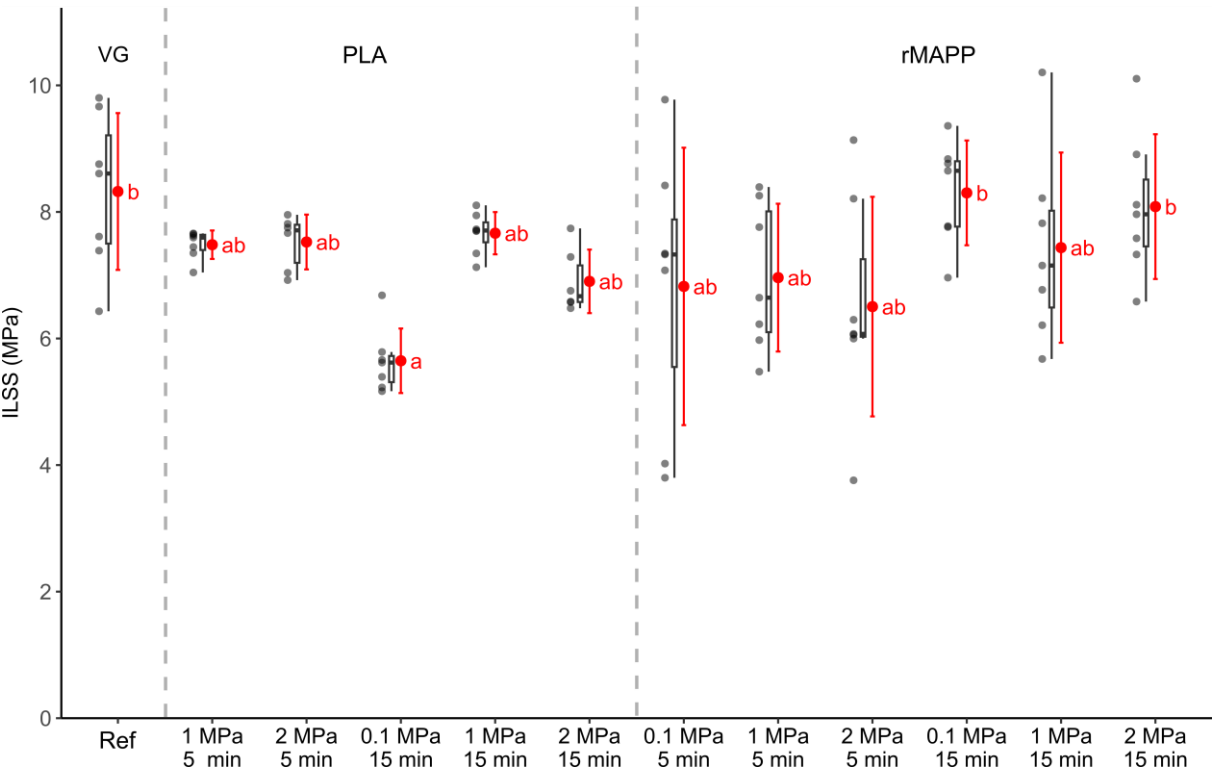


**Fig.4** ILSS of beech plywood manufactured with various combinations of additional heating time (AHT) in minutes and pressure in MPa using the three selected adhesives

**Fig.5** shows the ILSS results for Douglas-fir plywood. The overall findings reveal that most ILSS results obtained with rMAPP and PLA (marked with the letter “b”) do not exhibit a statistically significant difference compared to the VG reference test. The Kruskal-Wallis test indicates a statistically significant effect of adhesive choice and manufacturing parameters on the ILSS of the samples ( $p < 0.0006$ ). Further analysis using the corrected post-hoc Dunn’s test reveals that Douglas-fir samples glued with PLA at 1 and 2 MPa with an AHT of 15 minutes (marked with the letter “a”) are the only samples that do not belong to the same distribution as the VG reference sample.

The significant gap in ILSS values observed between the beech and Douglas fir samples is attributed to the inherent lower strength of Douglas fir wood compared to beech, as indicated in references [39, 40].

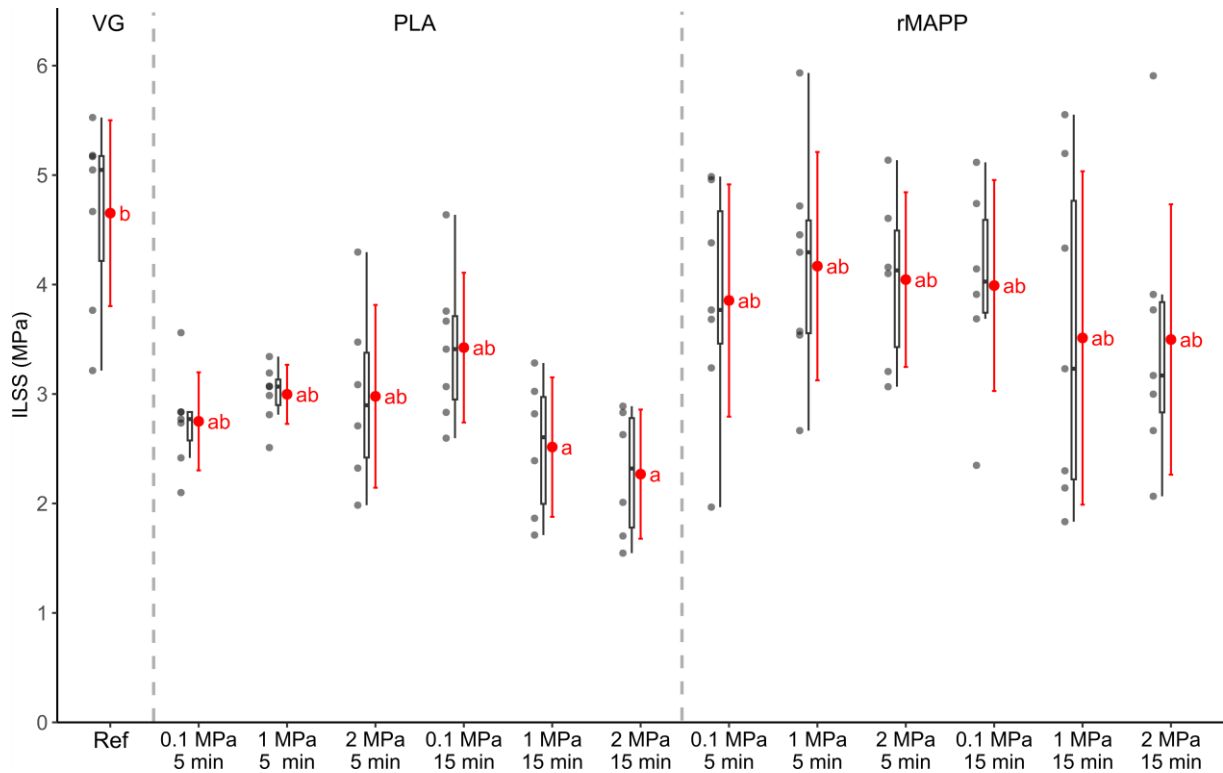


Fig.5 Interlaminar shear strength (ILSS) of Douglas plywood manufactured with various combinations of additional heating time (AHT) and pressure using the three selected adhesives

### Fracture mode and surface

Visual and microscopic observations are made to analyse the fracture surfaces after the tests and the samples are categorised according to their fracture modes. Some examples are presented in **Fig.6**. Six distinct fracture modes are identified: cohesive fracture located in the wood (Co-W (**Fig.6(a)**)), cohesive fracture located in the adhesive (Co-A (**Fig.6(b)**)), mix of adhesive fracture and cohesive fracture located in the adhesive (A/Co-A (**Fig.6(c)**)), mix of adhesive fracture, cohesive fracture located in the adhesive and cohesive fracture located in the wood (A/Co-A/Co-W(**Fig.6(d)**)), mix of cohesive fracture in the adhesive and cohesive fracture in the wood (Co-A/Co-W(**Fig.6(e)**)), and out of joint (OJ). Beech samples bonded with PLA primarily experience a mixed adhesive / cohesive adhesive mode (A/Co-A), with the adhesive being the limiting factor. In contrast, a majority of rMAPP-bonded samples exhibit cohesive fractures within the wood substrate (Co-W), making wood the limiting factor.

This difference in failure mechanisms alters the interpretation of the ILSS values for rMAPP-bonded samples, suggesting that these values represent the ILSS limit achievable at the interface, but not the maximum potential of the adhesive. This could also explain the difference in variability observed

between samples with ruptures located within the PLA joint and those within the veneer, with PLA displaying a lower variability in failure than wood [41].

The fracture analysis for Douglas fir samples (**Appendix 2**) indicates that most of the configurations result in cohesive fractures within the wood substrate (Co-W) or a mixed fracture involving the wood substrate. Consequently, the wood veneer emerges as the weak link in these ILSS tests, limiting the potential interpretations of the influence of the manufacturing parameters and the adhesive contribution to ILSS.

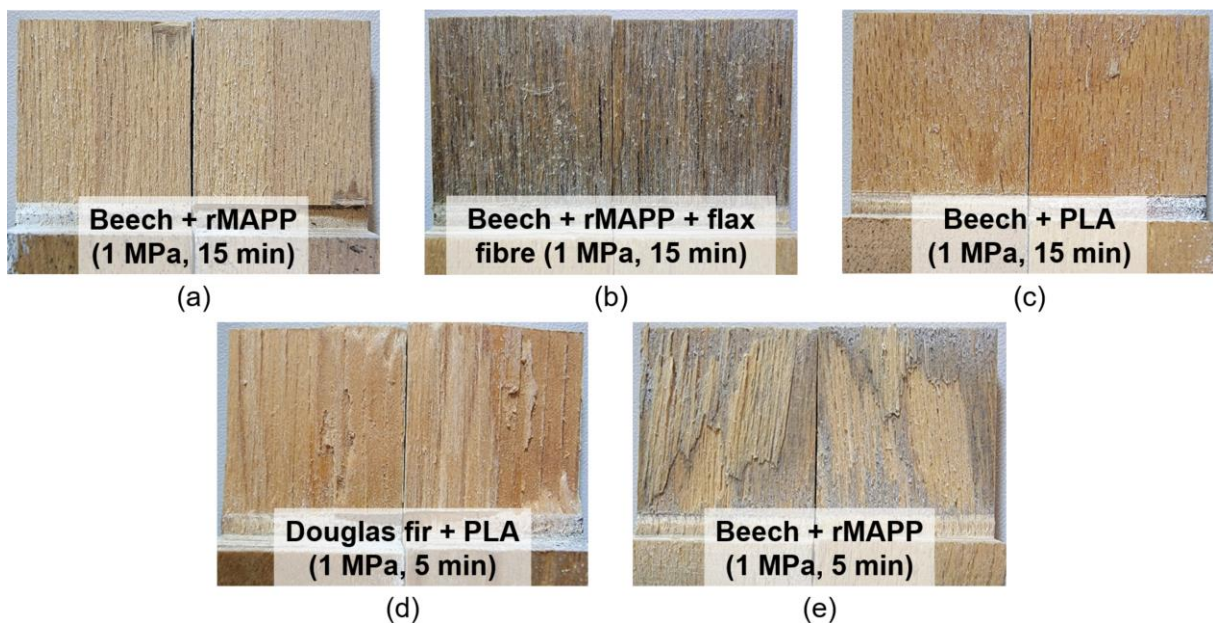


**Fig.6** Examples of fracture surfaces. (a): Co-W; (b): Co-A; (c): A/Co-A; (d): A/Co-A/Co-W; (e): Co-A/Co-W.

The difference in fracture behaviour can be attributed to the mechanical properties of the polymers themselves. At ambient temperature, PP remains in the rubbery state. Its softness and deformability facilitate the redistribution of stress within the bond line and throughout the surrounding veneers. In contrast, PLA is in a glassy state, exhibiting higher rigidity, brittleness and significantly lower capacity to deform, resulting in brittle fractures at the plywood interfaces. This phenomenon is observable on the stress-deflections curves of the ILSS tests presented in **Fig. 7**, as it showcases clear ruptures at lower deflection values for the samples glued with PLA, where samples glued with rMAPP reach a higher value of deflection, and demonstrate gradual break patterns.

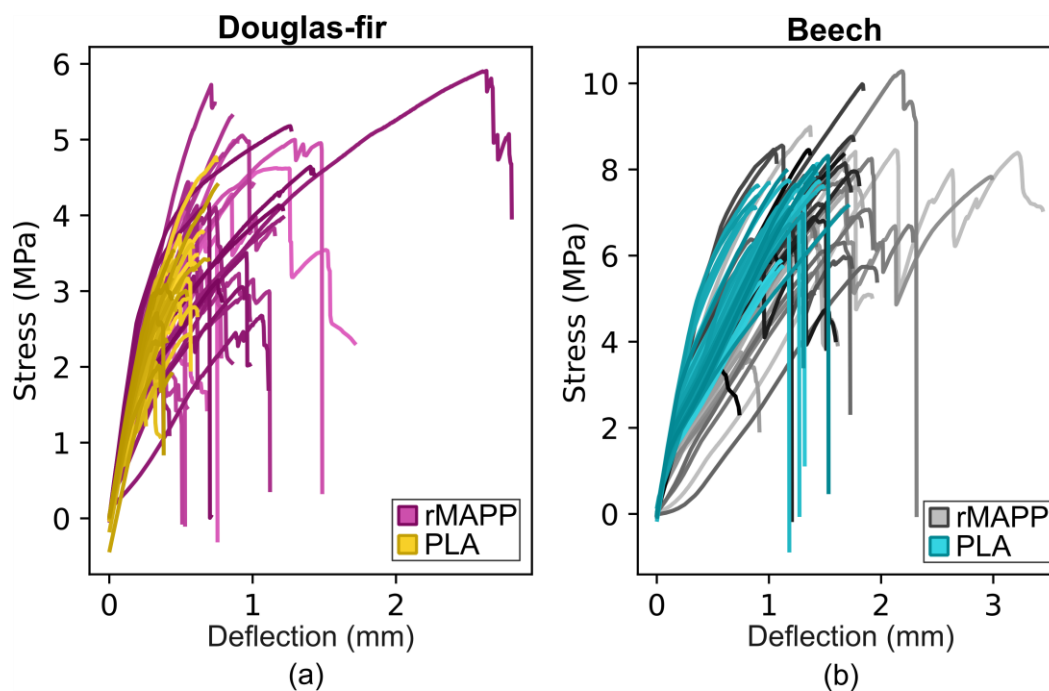


**Fig. 7** Stress-deflection curves for ILSS testing on douglas (a) and beech (b) samples bonded with rMAPP or PLA

Nonetheless, all these results point out the suitability of using PLA and rMAPP with these two wood species in plywood production, provided that appropriate manufacturing parameters are applied. This demonstrates their ability to effectively compete with the reference VG adhesive.

### Interphase region and bonding interactions

**Fig.8(a)** shows tomographic observations across the radial-tangential (RT) plane of the interface between the middle veneers (taken outside the joint region and away from the sample borders), for different wood species and adhesives. The images show characteristic anatomical features of wood. They are detailed with arrows. Certain wood vessels near the interface between the veneers appears to have a different colour compared to those further away from the interface. Vessels filled with rMAPP display a grey level brighter than air but darker than wood due to the lower density of rMAPP. Those filled with PLA are harder to distinguish from wood because the density of PLA is close to that of the wood. The green dotted lines delimit the boundaries of the area where some vessels are filled, referred to as the interphase region. A distinctive glue line varying in thickness depending on the type of adhesive and the species of wood, is highlighted by the brown line. These distinct areas are the same that those depicted in Castanié et al. [42]. Corresponding images on **Fig.8(b)** show the same visuals after machine learning segmentation using the Fiji plugin "Trainable Weka Segmentation". The aim of the segmentation is to highlight the adhesive, allowing a clearer view of its diffusion. In the displayed images, a higher level of brightness indicates a higher probability that a given pixel corresponds to the adhesive.

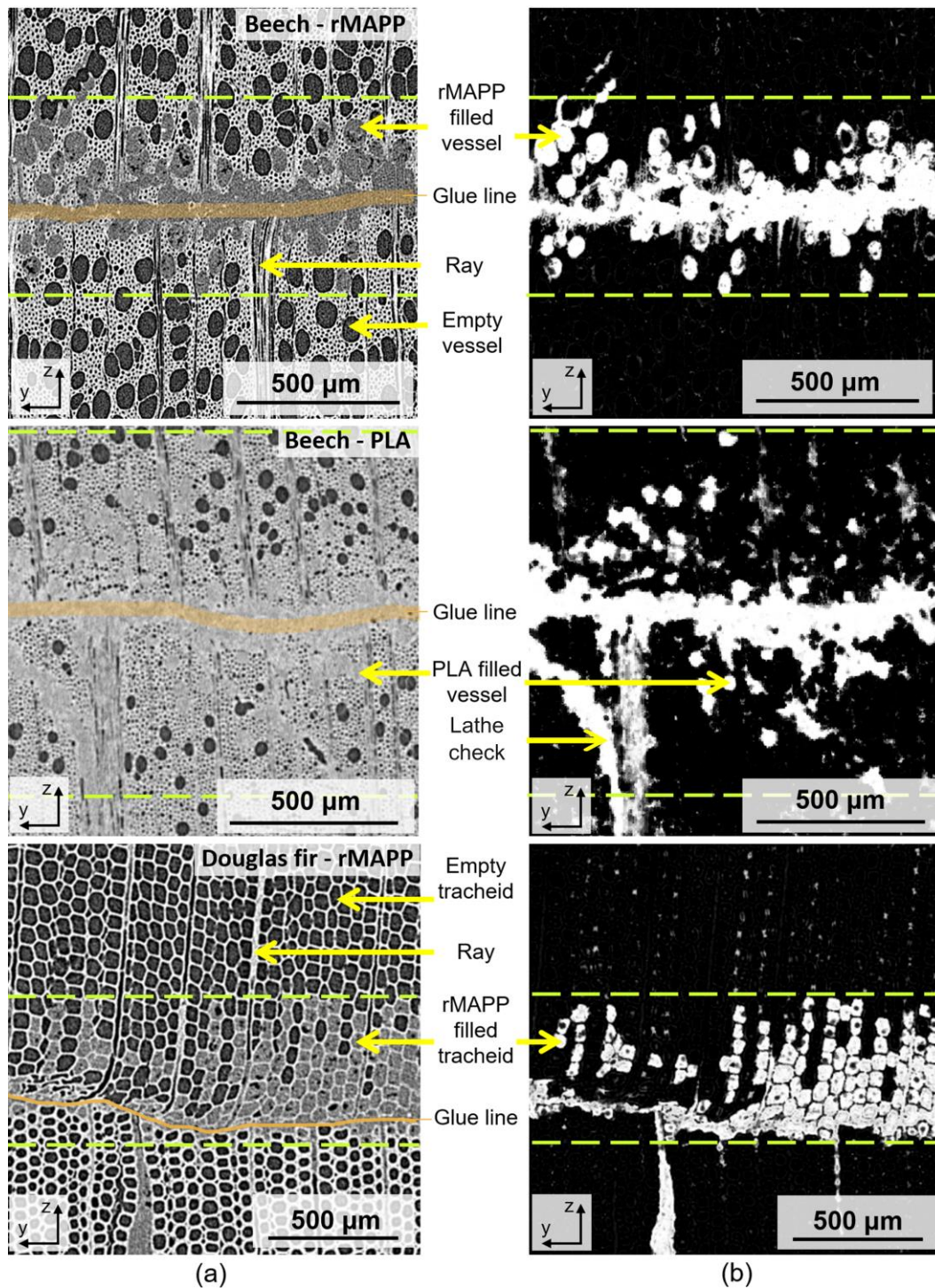


**Fig.8** (a) X-Ray cross section of samples middle interface. (b) X-Ray cross section slices of samples middle interface with highlighted adhesive through segmentation. The green dotted line marks the boundaries of the interphase region

The observed diffusion of adhesive within the vessels implies that the interfacial adhesion between veneer layers results not only from chemical bonding but also from mechanical interlocking.

Indeed, at a plywood interface, bonding interactions are typically categorised into two distinct types: chemical bonding and mechanical bonding.

Mechanical bonding encompasses macroscopic phenomena where mechanical stresses are applied to the veneer and/or the adhesive to uphold bond strength. Within a plywood interface, these bonds are observed through phenomena such as adhesive anchoring in cracks and damages, adhesive penetration in wood cell voids and surface roughness. Previous studies have shown, for example, that lathe checks, which are periodic cracks formed on the inner edge of the veneer during the peeling process, have a significant role in the mechanical performance of the joint [39, 40]. The presence of these mechanical anchoring points with the adhesive used is illustrated on **Fig.8**. This phenomenon is observed for all the tested materials.

The **Fig.8** also highlights some irregularities in the glue line depth, particularly noticeable in the Douglas-fir – rMAPP image, which increase the surface roughness. Surface roughness in veneers is well-known to be affected by the wood grain structure, the cutting technique, and the wood species, and can create additional mechanical anchoring points for the adhesive. Mechanical anchoring phenomena can also result from variations in surface hardness, influenced by the presence of earlywood or latewood or by wood anatomical features such as rays. During the fabrication process, the applied pressure on these irregularities can lead to surface interpenetration if a stiff feature encounters a softer part, as it is observable on the Douglas fir pictures on **Fig.8**. This effect is present in every tested sample, and therefore cannot be distinguished as an explanation for differences observed in interlaminar shear strength.

From the tomographic observation, it is evident that the adhesives penetrate into voids within the veneers, primarily within the vessel lumens. This phenomenon, also known as “bulk flow” [43], is influenced by factors such as lumen dimensions and openings on the wood surface, adhesive viscosity and surface energy, and process parameters including assembly time, temperature, pressure and moisture level [44]. This void penetration creates a new region around the adhesive joint, called the interphase region, visible in **Fig.8**, where mechanical properties are influenced both by the wood and the adhesive. The area seems to be wider for PLA glued samples, aligning with its lower viscosity compared to rMAPP, which may serve as a reinforcing element for the bond line, as demonstrated in the research conducted by Ebewe et al. [45].

Two distinct mechanisms facilitating the diffusion process are identified in the tested materials. The first one, prevalent in beech samples, involves diffusion from one vessel to another in close proximity, originating at the interface. This diffusion process has the potential to fill vessels with adhesive even in the absence of a direct connection to the interface. **Fig.9** illustrates this diffusion phenomenon with illustrations obtained by CT scan a beech plywood sample glued with rMAPP. Red area is determined by segmentation and illustrates areas filled with rMAPP, allowing the adhesive pathway through beech vessels to be seen.

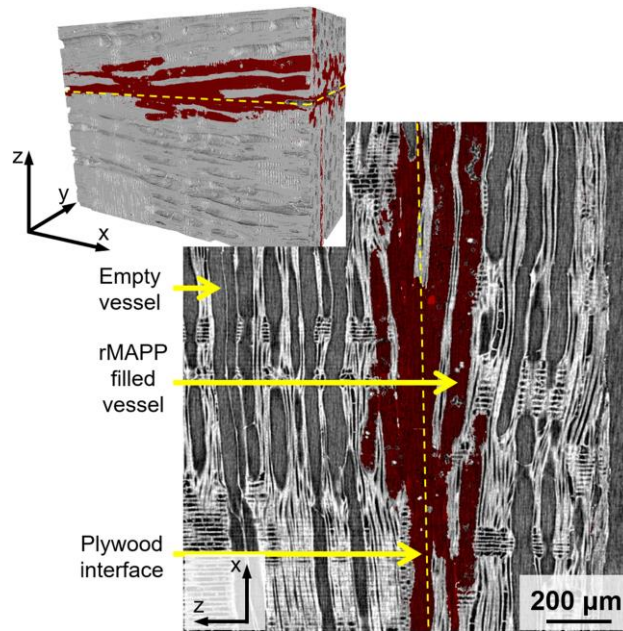


**Fig.9** X-Ray cross section and 3D reconstruction illustrating the adhesive diffusion through communicating and merging vessels. Plywood interface is marked by the yellow dotted line.

The second diffusion mechanism, predominant in Douglas fir samples, involves diffusion from one tracheid to another in close proximity, specifically through tracheid bordered pits. Bordered pits are micrometric pores in the cell walls of tracheids that facilitate sap transfer. **Fig. 10** shows tomographic slices in plan  $xy$  and  $yz$  of a plywood sample made of Douglas fir and glued with rMAPP, from different angles. The picture is shown before (**Fig. 10(a)**) and after (**Fig. 10(b)**) adhesive segmentation, represented by the red areas. The pointed cell wall has a porosity that allows the adhesive to flow. Its shape is that of a bordered pit border. The important difference in diffusion between earlywood (thin cell walls) and latewood (thicker cell walls) observed in the last image of **Fig.8(b)**, is due to the greater thickness of pits components in latewood than in earlywood, which reduces its permeability and therefore the adhesive diffusion [46].



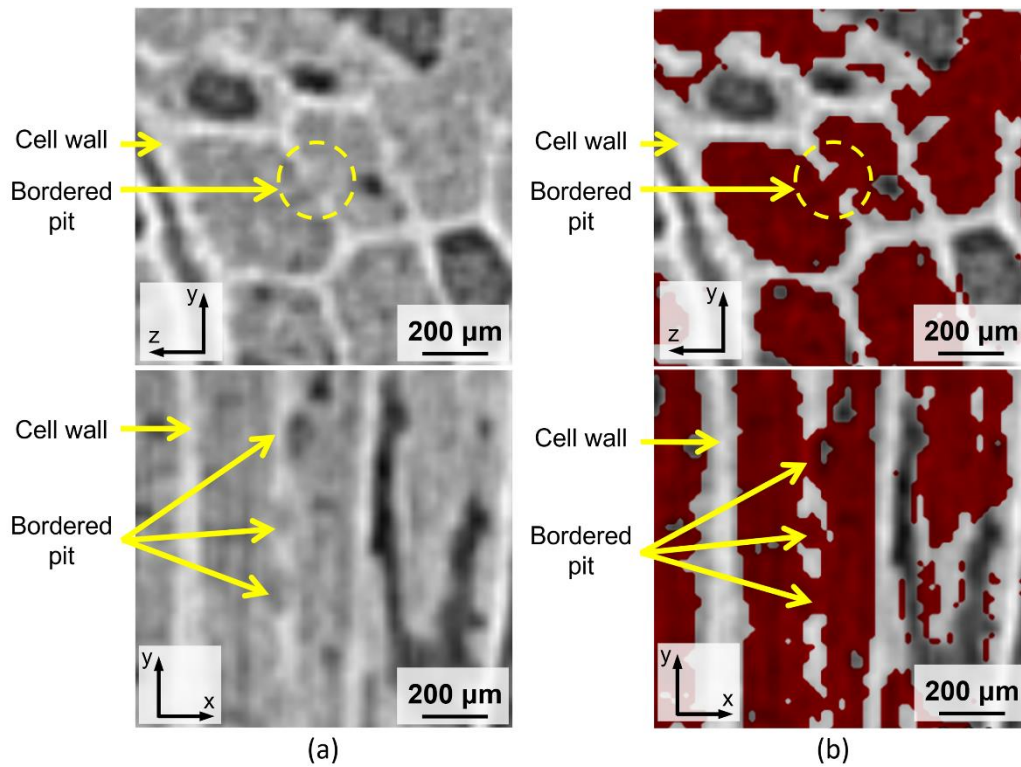


**Fig. 10** X-Ray cross-section illustrating adhesive diffusion through bordered pits in Douglas fir tracheids, before (a) and after (b) adhesive segmentation (red areas)

**Fig. 11** shows a 3D representation of the segmented adhesive layer, with the wood cell walls virtually hidden. The figure clearly illustrates how the resin fills the wood vessels, creating a strengthening network in the shape of cylindrical resin structures.

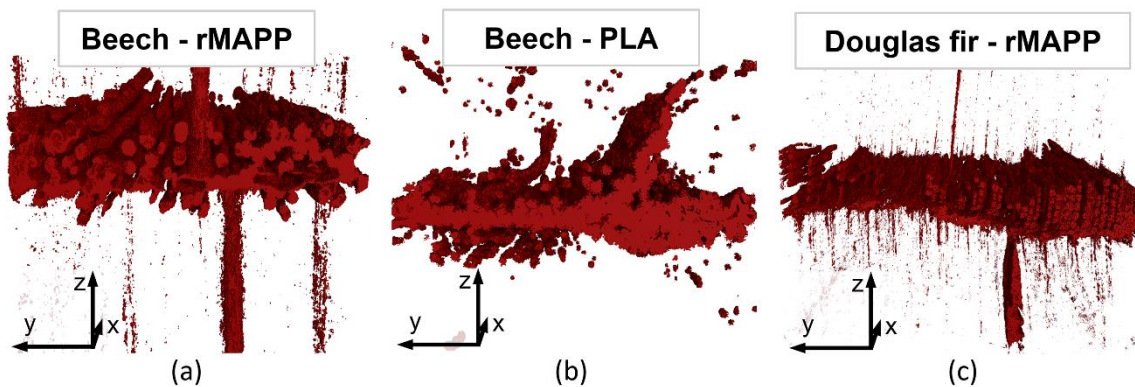


**Fig. 11** X-Ray 3D reconstructions of plywood adhesive bondline for different wood species and adhesive, illustrating adhesive diffusion in nearby vessels or tracheids

The interlocking mechanism may explain the higher incidence of cohesive fracture in rMAPP bonded samples. An alternative explanation may lie in the brittle nature of the PLA adhesive, which exhibits around 5% strain at break, in contrast to the highly ductile behaviour of rMAPP, which exhibits 918 % strain at break.

The advantageous aspect of adhesive diffusion into nearby empty vessels of the veneer lies in its facilitation of improved stress distribution and reinforcement of the vessels [43]. However, while studies have demonstrated that penetration depth can have a beneficial effect on the bond strength [45], excessive diffusion can lead to the formation of an overly small bond joint, known as “starved” joint, which ultimately weakens the interface bonding [47]. In the present study, the CT scan observations reveal that the bond line remains significant for beech samples, whereas is considerably smaller for the Douglas-fir samples. However, the great majority of wood-cohesive fracture mode in the Douglas-fir indicates that their bond line thickness is sufficient to not be the limiting factor.

Another potential mechanical bonding phenomenon is macro-molecular entanglement, which unfortunately remains undetectable in tomographic observations due to insufficient resolution. This phenomenon may involve the entangling of polymer chains derived from the amorphous constituents of the cell walls themselves [48] or between these chains and those of the adhesive [49]. Further ultrastructural analysis would be required to shed light on the existence of these potential mechanisms in the studied materials.

Despite the observed differences in the mechanical anchorage mechanisms between the two wood veneer types and the two adhesives, the most plausible hypothesis to explain the higher ILSS values obtained for rMAPP with both wood species is related to chemical bonding. Indeed, chemical bonding phenomena play a decisive role in the final strength of the bond line [44]. In the case of rMAPP, covalent bonds are formed through esterification between the maleic anhydride and the hydroxyl groups of the amorphous constituents of the wood cell wall. Additionally, hydrogen bonds can be formed between the hydroxyl group of unoccupied sites. For PLA bonded veneers, the only bonds created are hydrogen bonds between the hydroxyl groups of amorphous constituents of the wood cell walls and the polar oxygen in the PLA molecule. Although hydrogen bonding is among the strongest intermolecular forces, it remains much weaker than covalent bonds. Moreover, it is susceptible to hydrophilicity, as bonds formed with hemicellulose or amorphous cellulose can be displaced by water molecules.

Finally, a last hypothesis could be put forward to explain the observed differences in adhesion between the different tested materials. This involves the infiltration of the polymer into the wood cell wall. This phenomenon has been shown to have a significant impact on the bond strength [50]. However, it can only occur if the monomers possess a sufficiently low molecular weight, therefore favouring adhesive with *in-situ* polymerisation [51]. In the studied thermoplastic adhesives, polymer chains undergo pre-polymerization before veneer assembly, resulting in a molecular weight that is too high for diffusion into the cell walls during veneer bonding.

**Fig. 12** presents a schematic representation of the described bonding interactions occurring within the interface region of the adhesive-bonded veneers.

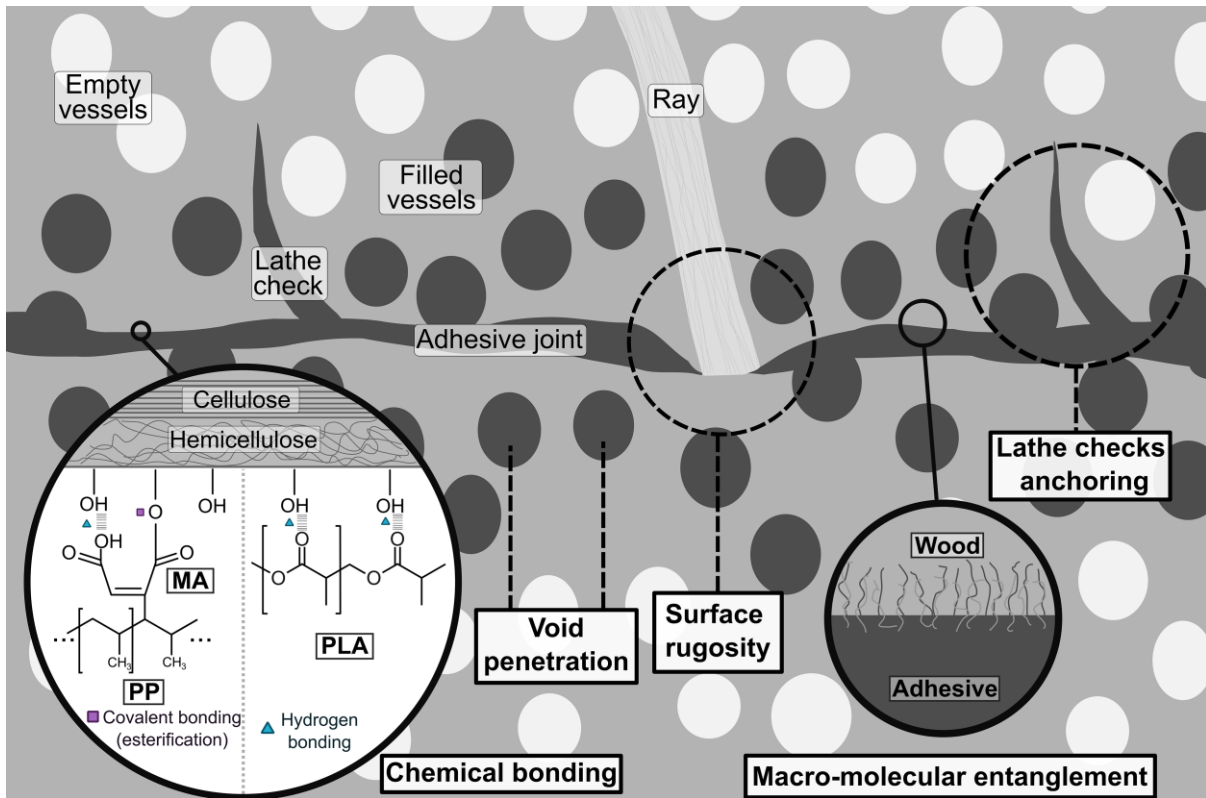


**Fig. 12** Representation of the different bonding phenomena occurring in the plywood interface

### 3.2. Influence of the incorporation of UD flax fibres in the adhesive

#### Interlaminar shear strength

**Fig.13** displays the results obtained from ILSS tests conducted on the plywood interface, bonded with PLA and rMAPP, reinforced with unidirectional flax fibres oriented either parallel or perpendicularly to the wood grain, (detailed results are provided in **Appendix 1.**). Results showing statistically significant means difference are marked by a different letter.

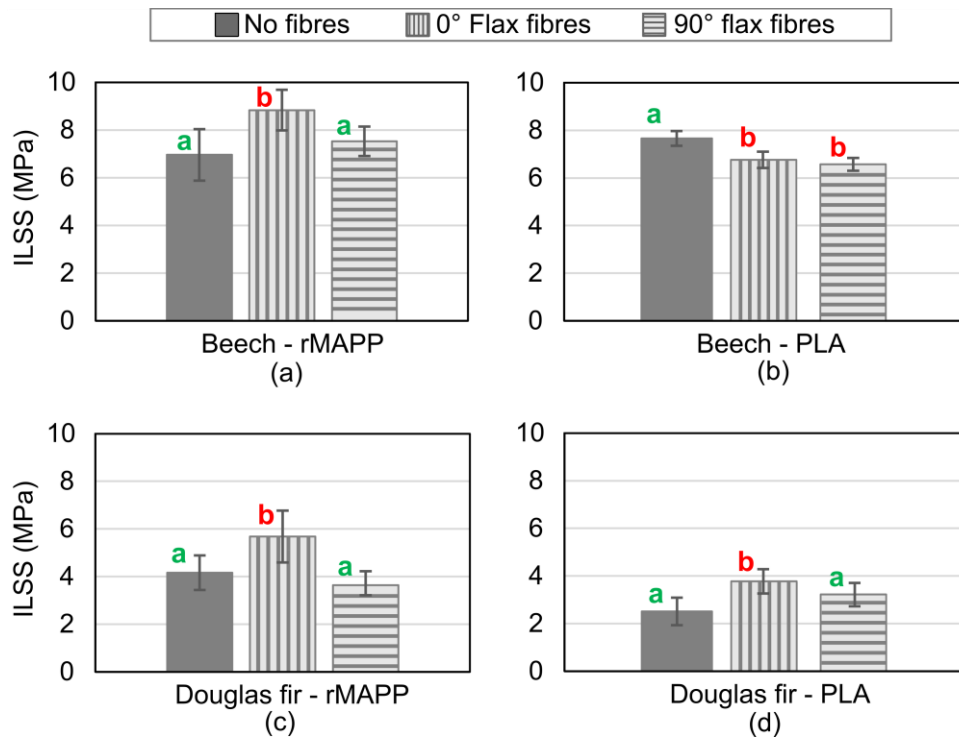


**Fig.13** ILSS of beech and Douglas fir plywood bonded with PLA and rMAPP, with or without flax fibre reinforcement.

In the case of beech plywood bonded with rMAPP, the addition of flax fibres at 0° resulted in a statistically significant improvement of ILSS ( $p < 0.007$ ), increasing from 6.96 MPa to 8.83 MPa (+27%). However, the addition of fibres with a 90° orientation do not yield significant variation ( $p > 0.3$ ). For beech plywood bonded with PLA, the incorporation of fibres leads to a significant reduction in ILSS ( $p < 0.0005$ ), from 7.66 MPa to 6.76 MPa (-12%). A similar effect is observed for fibres oriented at 90°, with ILSS decreasing from 7.66 MPa to 6.57 MPa (-14%). This can be attributed to the fact that PLA also forms hydrogen bonds with the flax fibres, which do not contribute to shear strengthening the bond line. The observations regarding the fibre reinforcement effect in this study differ from those reported by Jorda et al. [21] on beech plywood glued with urea-formaldehyde (UF) and reinforced with flax fibres, where no significant effect was observed. Several possible reasons can account for these discrepancies. A possible explanation could be the lower areal weight of fibre reinforcements used in their study, at 50 g/m<sup>2</sup>, as this may not provide sufficient reinforcement to significantly strengthen the interface. Another factor to consider is the adhesive used. In the current study, samples bonded with rMAPP show an increase in ILSS when reinforced with flax fibres, whereas samples bonded with PLA do not, as does the UF adhesive in the study by Jorda et al. [21]. The improved performance with fibre reinforcement may be attributed to the better adhesive properties of rMAPP and its compatibility with cellulosic materials due to the maleic anhydride grafting, which may have enhanced the interaction between the adhesive, fibres, and wood substrates.

When it comes to Douglas fir samples, those glued with rMAPP exhibit a significant increase in ILSS ( $p < 0.04$ ) when 0° fibres are added, increasing from 4.17 MPa to 5.69 MPa (+36%). However, no

statistically significant effect is observed when fibres are oriented at a 90° angle. ILSS values for Douglas fir samples glued with PLA significantly increased ( $p < 0.007$ ) when fibres with a 0° orientation were added, rising from 2.52 MPa to 3.77 MPa (+50%). For fibres oriented at 90°, there is no significant variation in ILSS ( $p > 0.06$ ).

### **Fracture mode and surface**

The presence of flax fibres at the interface appears to have a significant effect on the fracture modes of rMAPP and PLA glued beech plywood, predominantly leading to cohesive fractures occurring within the adhesive (Co-A). However, this effect is not observed in Douglas fir plywood, where cohesive fracture within the wood (Co-W) remains predominant.

### **Interphase region**

**Fig.14** shows a microscopic observation (a and b) and a X-ray slice (c) of the transverse cross-section of a sample of beech plywood glued with rMAPP, with and without flax fibre reinforcement. In the microscopic observation of the non-reinforced sample (**Fig.14(a)**), adhesive diffusion into the nearby vessels is observed. When flax fibres are added at the interface (**Fig.14(b), (c)**), they form a joint approximately 100 µm thick. Interestingly, the phenomenon of adhesive diffusion into nearby veneers is still present, even though most of the adhesive serves as matrix for the flax fibres.

Observation of the fracture surfaces of reinforced and non-reinforced plywoods shows a correlation between joint composition and interface failure mode. Beech samples reinforced with flax fibres have a higher occurrence of cohesive fractures within the adhesive compared to non-reinforced ones. This can be attributed to the thicker and stiffer joint in reinforced plywoods, enabling shear stress concentration within the composite joint and reducing stress on the wood veneer. The fracture mode observed suggests that these results can be interpreted as shear strength of the adhesive rather than being limited by the strength of wood veneers. In contrast, Douglas-fir samples reinforced with flax fibre show no difference in fracture mode despite a thicker joint. The difference with beech samples may be due to the lower strength of Douglas-fir, which causes the veneer to break before the reinforced adhesive reaches its limit. No fibre bridging was observed in the tested materials.

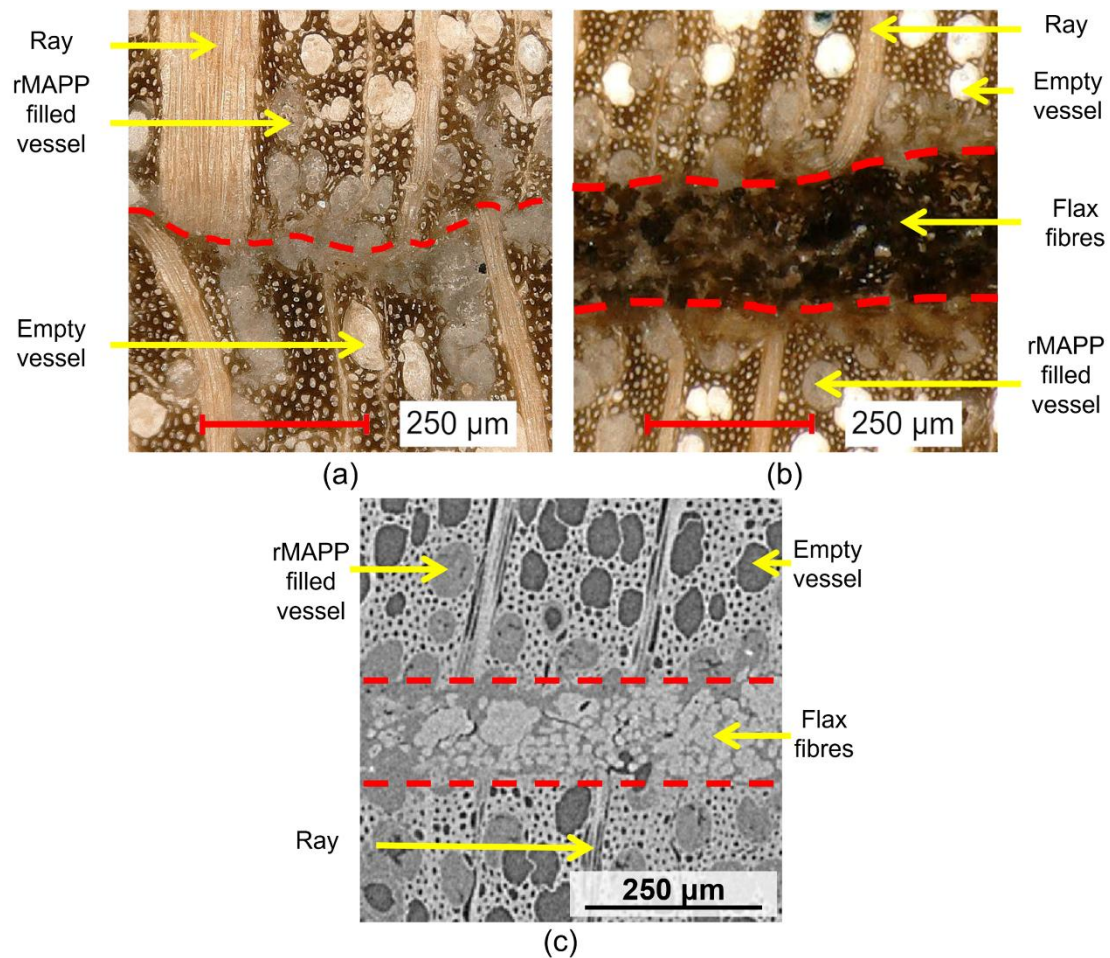


**Fig.14** - Cross-cut microscopic observations of beech samples middle interface, glued with rMAPP. (a) and (b) are obtained with a numerical microscope, (c) is a cross section obtained through X-Ray CT Scanning. Samples on (b) and (c) have flax fibre reinforcement at its middle interface. The red dotted lines delimit the border of the bond line

### 3.3. Effect of ageing on ILSS

The ILSS of samples made with the different veneer species, adhesives and stratifications is also measured after undergoing accelerated ageing processes. The aim is to gain insight into the ageing behaviour of the interfaces and the effect of the incorporation of flax fibres between the veneers on the ageing behaviour. The overall results are presented in **Appendix 2**.

In **Fig.15**, ILSS results for the “Ag1” ageing campaign (40 days at 40 °C 90% RH) are presented. Samples of beech plywood glued with rMAPP shows a statistically significant increase ( $p < 0.0009$ ) in ILSS following this ageing, rising from 6.96 MPa to 9.43 MPa (+35%). This improvement could be due to a relaxation of residual stresses accumulated during manufacture and reconditioning because of the relative humidity variations of the plywood.

When flax fibres are present between the middle veneers, the ageing leads to a significant decrease ( $p < 0.0004$ ) in ILSS, dropping from 8.83 MPa to 6.63 MPa (-25%). This decrease could be caused by interface degradation between the natural fibres and the adhesive due to the swelling and shrinking of

the fibres during the ageing and reconditioning processes, as presented by Assarar et al. [28] for plant fibre composites.

In the case of beech veneers glued with PLA, the ageing process has a detrimental effect on the ILSS values, regardless of the presence of flax fibres. Without the fibres, the ILSS value significantly decreases ( $p < 0.0004$ ) from 7.66 MPa to 6.48 MPa (-15%). With the fibres, ILSS decreases from 6.76 MPa to 4.82 MPa (-38%). This reduction is attributed to the plasticizing effect of water on PLA and wood cell wall, to the onset of PLA degradation due to the hydrolysis phenomenon, coupled with fibre/matrix interface degradation due to fibre swelling. The water molecules infiltrate both in PLA and wood cell amorphous components, forming hydrogen bonds that replace those initially formed between PLA and cell wall components, potentially increasing flexibility at the interface.

Interestingly, samples of Douglas fir plywood glued with rMAPP shows no statistically significant variations in ILSS after ageing, whether flax fibres are present or not ( $p > 0.9$  and  $p > 0.3$ ). When the Douglas fir veneers are glued with PLA, ageing has no significant effect ( $p > 0.05$ ) on the ILSS value. However, an effect is observed when samples have flax fibres between their middle veneers, resulting in a significant decrease ( $p < 0.004$ ) from 3.77 MPa to 2.82 MPa (-25%).

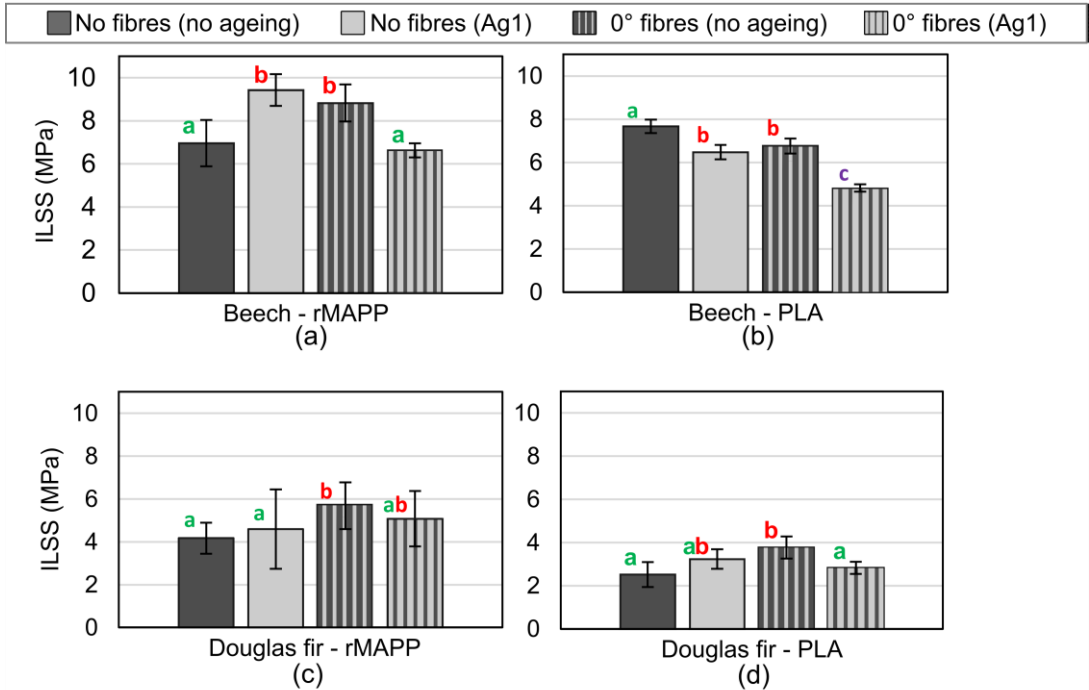


**Fig.15** - Interlaminar shear strength of reinforced and non-reinforced plywood before and after Ag1 ageing

The effects of immersion accelerated ageing (Ag 2) on the ILSS of beech and Douglas fir plywood are presented in **Fig.16**. It is worth noting that samples bonded with PLA show rapid debonding due to adhesive hydrolysis during the ageing process, therefore the results are not presented.

For beech samples glued with rMAPP, the ageing process results in a statistically significant improvement ( $p < 0.05$ ) of the shear strength, with an increase of the ILSS value from 6.96 MPa to 9.16 MPa (+32%). The decrease in number of hydroxyl groups in wood cell constituents resulting from the formation of covalent bonds via esterification with maleic anhydride, along with the coating of cell wall surfaces by the hydrophobic chains of PP, account for the material's excellent resistance to ageing. When flax fibres are present at the interface, the ageing process leads to a significant decrease ( $p < 0.00001$ ) in ILSS, dropping from 8.83 MPa to 4.47 MPa (-49%).

In the case of Douglas fir samples glued with rMAPP, there is no significant variation ( $p > 0.7$ ) observed when subjected to the ageing process. However, Douglas fir samples reinforced with flax fibre experience a significant decrease ( $p < 0.002$ ) in ILSS from 5.69 MPa to 2.94 MPa (-48%).

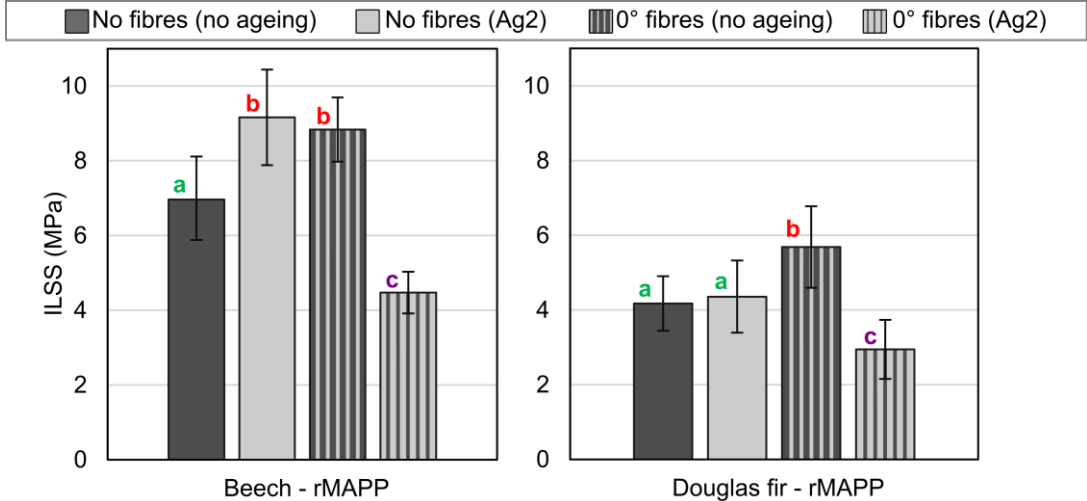


**Fig.16** - Interlaminar shear strength of reinforced and non-reinforced plywood before and after Ag1 ageing

Ageing does not have a significant effect on the fracture behaviour of beech plywood bonded with rMAPP. For non-reinforced samples, the fracture mode still involves at least partial engagement with the wood veneers, making it challenging to draw conclusions regarding adhesive alteration. In contrast, reinforced beech samples glued with rMAPP continue to fracture mainly within the adhesive joint even after ageing. The significant decrease in their ILSS values following ageing can be attributed to interface degradation, possibly arising from fibre/matrix interface degradation [28].

Aged Douglas-fir samples mostly experience fractures that occur fully or partly within the wood veneer. This outcome does not provide sufficient evidence to draw conclusions about the potential effects of ageing on the interface performance.



## 4. Conclusion

The aim of this study was to evaluate the performance of thermoplastic resins, specifically rMAPP and PLA, as adhesives in plywood made of beech and second-grade Douglas fir veneers. These evaluations were carried out with or without flax fibre reinforcement and the study utilised interlaminar shear strength testing before and after ageing. The results show that both rMAPP and PLA exhibited ILSS values within the range of a standard vinyl adhesive as a reference. This suggests that both rMAPP and PLA have the potential to serve as efficient formaldehyde-free adhesives for plywood production. Additionally, rMAPP demonstrated excellent ageing resistance attributed to its hydrophobic nature, making it suitable for outdoor applications. In contrast, PLA displayed a poor ageing resistance due to its biodegradable nature, limiting its suitability to indoor applications. X-ray tomography observations allowed to highlight the different adhesion mechanisms occurring in the bond line and demonstrating the role of mechanical anchoring in the overall behaviour of the joint.

The addition of fibre reinforcement significantly improved ILSS for beech and Douglas fir plywood glued with rMAPP and for Douglas plywood glued with PLA. However, its effect was insignificant for beech plywood glued with PLA. When the reinforced plywood samples were aged, they exhibited a lower ILSS value compared to their unaged and unreinforced counterparts. This decrease is attributed to the probable interfacial degradation between the fibres and the matrix during the ageing and drying cycles. Plant fibre reinforcement proves to be an effective means of improving ILSS performance, but it should be limited to indoor plywood applications.

This study has shown that recycled (rMAPP) and bio-based (PLA) thermoplastics are viable alternatives to traditional petroleum-based adhesives in plywood production. The choice between these adhesives should be based on the intended application environment. Moreover, fibre reinforcement stands out as a relevant option to improve the interfacial performance in plywoods.

## 5. Acknowledgements

This work was supported by the "Investissements d'Avenir" program, ISITE-BFC project (ANR-15-IDEX-0003 contract) as part of the WooFHi project and by EIPHI Graduate School under ("ANR-17-EURE-0002"). Authors are grateful to MIFHySTO technological platform (FEMTO-ST, France) for the use of X-ray nanotomography. We also sincerely wish to thank Louis Denaud, Guillaume Pot, Jean-Claude Butaud, Stéphane Girardon and Leyne Demoulin from the WMM (Wood Material and Machining) team at LaBoMaP research lab (Cluny, France) for providing the veneers and for the insightful discussions conducted within the framework of the WooFHi project on veneer peeling and the properties of wood veneers.

## **6. Declarations**

### **Conflict of interest**

The authors declare that they have no conflict of interest.

### **Data and code availability**

The datasets analyzed during the current study will be made available upon reasonable request.

### **Supplementary information**

Not applicable.

### **Ethical approval**

Not applicable.

## 7. Bibliography

- [1] Substance Evaluation Conclusion as required by REACH Article 48 and Evaluation Report for FORMALDEHYDE.pdf. (n.d.)
- [2] Ferdosian, F.; Pan, Z.; Gao, G.; Zhao, B. (2017). Bio-Based Adhesives and Evaluation for Wood Composites Application, *Polymers*, Vol. 9, No. 12, 70. doi:10.3390/polym9020070
- [3] Mansouri, N.-E. E.; Pizzi, A.; Salvado, J. (2007). Lignin-based polycondensation resins for wood adhesives, *Journal of Applied Polymer Science*, Vol. 103, No. 3, 1690–1699. doi:10.1002/app.25098
- [4] Gonçalves, D.; Bordado, J. M.; Marques, A. C.; Galhano dos Santos, R. (2021). Non-Formaldehyde, Bio-Based Adhesives for Use in Wood-Based Panel Manufacturing Industry—A Review, *Polymers*, Vol. 13, No. 23, 4086. doi:10.3390/polym13234086
- [5] Ang, A. F.; Ashaari, Z.; Lee, S. H.; Md Tahir, P.; Halis, R. (2019). Lignin-based copolymer adhesives for composite wood panels – A review, *International Journal of Adhesion and Adhesives*, Vol. 95, 102408. doi:10.1016/j.ijadhadh.2019.102408
- [6] Antov, P.; Savov, V.; Neykov, N. (2020). SUSTAINABLE BIO-BASED ADHESIVES FOR ECO-FRIENDLY WOOD COMPOSITES. A REVIEW, *WOOD RESEARCH*, 15
- [7] Geng, X.; Li, K. (2006). Investigation of wood adhesives from kraft lignin and polyethylenimine, *Journal of Adhesion Science and Technology*, Vol. 20, No. 8, 847–858. doi:10.1163/156856106777638699
- [8] Li, K.; Geng, X.; Simonsen, J.; Karchesy, J. (2004). Novel wood adhesives from condensed tannins and polyethylenimine, *International Journal of Adhesion and Adhesives*, Vol. 24, No. 4, 327–333. doi:10.1016/j.ijadhadh.2003.11.004
- [9] Bekhta, P.; Müller, M.; Hunko, I. (2020). Properties of Thermoplastic-Bonded Plywood: Effects of the Wood Species and Types of the Thermoplastic Films, *Polymers*, Vol. 12, No. 11, 2582. doi:10.3390/polym12112582
- [10] Kajaks, J.; Kalnins, K.; Reihmane, S.; Bernava, A. (2014). Recycled Thermoplastic Polymer Hot Melts Utilization for Birch Wood Veneer Bonding, *Progress in Rubber, Plastics and Recycling Technology*, Vol. 30, No. 2, 87–102. doi:10.1177/147776061403000202
- [11] Song, W.; Wei, W.; Li, X.; Zhang, S. (2016). Utilization of Polypropylene Film as an Adhesive to Prepare Formaldehyde-free, Weather-resistant Plywood-like Composites: Process Optimization, Performance Evaluation, and Interface Modification, *BioResources*, Vol. 12, No. 1, 228–254. doi:10.15376/biores.12.1.228-254
- [12] Gaugler, M.; Luedtke, J.; Grigsby, W. J.; Krause, A. (2019). A new methodology for rapidly assessing interfacial bonding within fibre-reinforced thermoplastic composites, *International Journal of Adhesion and Adhesives*, Vol. 89, 66–71. doi:10.1016/j.ijadhadh.2018.11.010
- [13] Luedtke, J.; Gaugler, M.; Grigsby, W. J.; Krause, A. (2019). Understanding the development of interfacial bonding within PLA/wood-based thermoplastic sandwich composites, *Industrial Crops and Products*, Vol. 127, 129–134. doi:10.1016/j.indcrop.2018.10.069

- [14] Grigsby, W. J.; Puri, A.; Gaugler, M.; Lüedtke, J.; Krause, A. (2020). Bonding Wood Veneer with Biobased Poly(Lactic Acid) Thermoplastic Polyesters: Potential Applications for Consolidated Wood Veneer and Overlay Products, *Fibers*, Vol. 8, No. 8, 50. doi:10.3390/fib8080050
- [15] Bal, B. C.; Bektaş, İ.; Mengeloğlu, F.; Karakuş, K.; Ökkeş Demir, H. (2015). Some technological properties of poplar plywood panels reinforced with glass fiber fabric, *Construction and Building Materials*, Vol. 101, 952–957. doi:10.1016/j.conbuildmat.2015.10.152
- [16] Jorda, J.; Kain, G.; Barbu, M.-C.; Petutschnigg, A.; Král, P. (2021). Influence of Adhesive Systems on the Mechanical and Physical Properties of Flax Fiber Reinforced Beech Plywood, *Polymers*, Vol. 13, No. 18, 3086. doi:10.3390/polym13183086
- [17] Xu, H.; Nakao, T.; Tanaka, C.; Yoshinobu, M.; Katayama, H. (1998). Effects of fiber length and orientation on elasticity of fiber-reinforced plywood, *Journal of Wood Science*, Vol. 44, No. 5, 343–347. doi:10.1007/BF01130445
- [18] Kramár, S.; Trcala, M.; Chitbanyong, K.; Král, P.; Puangsin, B. (2020). Basalt-Fiber-Reinforced Polyvinyl Acetate Resin: A Coating for Ductile Plywood Panels, *Materials*, Vol. 13, No. 1, 49. doi:10.3390/ma13010049
- [19] Choi, S. W.; Li, M.; Lee, W. I.; Kim, H. S. (2014). Analysis of buckling load of glass fiber/epoxy-reinforced plywood and its temperature dependence, *Journal of Composite Materials*, Vol. 48, No. 18, 2191–2206. doi:10.1177/0021998313495071
- [20] Arya, S.; Kumar, R.; Chauhan, S.; Kelkar, B. U. (2023). Development of natural fiber reinforced thermoplastic bonded hybrid wood veneer composite, *Construction and Building Materials*, Vol. 368, 130459. doi:10.1016/j.conbuildmat.2023.130459
- [21] Jorda, J.; Kain, G.; Barbu, M.-C.; Köll, B.; Petutschnigg, A.; Král, P. (2022). Mechanical Properties of Cellulose and Flax Fiber Unidirectional Reinforced Plywood, *Polymers*, Vol. 14, No. 4, 843. doi:10.3390/polym14040843
- [22] ANSI-HPVA-HP-1 2020. (2020), American National Standards Institute
- [23] Banjo, A. D.; Agrawal, V.; Auad, M. L.; Celestine, A.-D. N. (2022). Moisture-induced changes in the mechanical behavior of 3D printed polymers, *Composites Part C: Open Access*, Vol. 7, 100243. doi:10.1016/j.jcomc.2022.100243
- [24] Yang, H.-S.; Wolcott, M. P.; Kim, H.-S.; Kim, S.; Kim, H.-J. (2007). Effect of different compatibilizing agents on the mechanical properties of lignocellulosic material filled polyethylene bio-composites, *Composite Structures*, Vol. 79, No. 3, 369–375. doi:10.1016/j.compstruct.2006.02.016
- [25] Felix, J. M.; Gatenholm, P. (1991). The nature of adhesion in composites of modified cellulose fibers and polypropylene, *Journal of Applied Polymer Science*, Vol. 42, No. 3, 609–620. doi:10.1002/app.1991.070420307
- [26] Demirkir, C.; Colakoglu, G.; Colak, S.; Aydin, I.; Candan, Z. (2016). Influence of Aging Procedure on Bonding Strength and Thermal Conductivity of Plywood Panels, *Acta Physica Polonica A*, Vol. 129, No. 6, 1230–1234. doi:10.12693/APhysPolA.129.1230
- [27] Senalik, C. A.; Ross, R.; Zelinka, S.; Lebow, S.; Cai, Z. (2017). Accelerated aging of preservative-treated structural plywood

- [28] Assarar, M.; Scida, D.; El Mahi, A.; Poilâne, C.; Ayad, R. (2011). Influence of water ageing on mechanical properties and damage events of two reinforced composite materials: Flax–fibres and glass–fibres, *Materials & Design*, Vol. 32, No. 2, 788–795. doi:10.1016/j.matdes.2010.07.024
- [29] Ghasemzadeh-Barvarz, M.; Duchesne, C.; Rodrigue, D. (2015). Mechanical, water absorption, and aging properties of polypropylene/flax/glass fiber hybrid composites, *Journal of Composite Materials*, Vol. 49, No. 30, 3781–3798. doi:10.1177/0021998314568576
- [30] Geyer, R.; Jambeck, J. R.; Law, K. L. (2017). Production, use, and fate of all plastics ever made, *Science Advances*, Vol. 3, No. 7, e1700782. doi:10.1126/sciadv.1700782
- [31] Plastics Europe. (2022). *PE-PLASTICS-THE-FACTS\_FINAL\_DIGITAL-1*
- [32] Ellis, W. D.; O’Dell, J. L. (1999). Wood-polymer composites made with acrylic monomers, isocyanate, and maleic anhydride, *Journal of Applied Polymer Science*, Vol. 73, No. 12, 2493–2505. doi:10.1002/(SICI)1097-4628(19990919)73:12<2493::AID-APP18>3.0.CO;2-C
- [33] Vink, E. T. H.; Rábago, K. R.; Glassner, D. A.; Gruber, P. R. (2003). Applications of life cycle assessment to NatureWorks™ polylactide (PLA) production, *Polymer Degradation and Stability*, Vol. 80, No. 3, 403–419. doi:10.1016/S0141-3910(02)00372-5
- [34] Skoczinski, P.; Carus, M.; Tweddle, G.; Ruiz, P.; Hark, N.; Zhang, A.; De Guzman, D.; Ravenstijn, J.; Käß, H.; Raschka, A. (2024). *Bio-based Building Blocks and Polymers – Global Capacities, Production and Trends 2023–2028* nova-Institut GmbH. doi:10.52548/VXTH2416
- [35] Van de Velde, K.; Baetens, E. (2001). Thermal and Mechanical Properties of Flax Fibres as Potential Composite Reinforcement, *Macromolecular Materials and Engineering*, Vol. 286, No. 6, 342–349. doi:10.1002/1439-2054(20010601)286:6<342::AID-MAME342>3.0.CO;2-P
- [36] Avat, F. (1993). Contribution à l’étude des traitements thermiques du bois jusqu’à 300°C: Transformations chimiques et caractérisations physico-chimiques, 363
- [37] Scida, D.; Assarar, M.; Poilâne, C.; Ayad, R. (2013). Influence of hygrothermal ageing on the damage mechanisms of flax-fibre reinforced epoxy composite, *Composites Part B: Engineering*, Vol. 48, 51–58. doi:10.1016/j.compositesb.2012.12.010
- [38] Kajaks, J.; Reihmane, S.; Grinbergs, U.; Kalnins, K. (2012). Use of innovative environmentally friendly adhesives for wood veneer bonding, *Proceedings of the Estonian Academy of Sciences*, Vol. 61, No. 3, 207. doi:10.3176/proc.2012.3.10
- [39] Viguier, J.; Bourreau, D.; Bocquet, J.-F.; Pot, G.; Bléron, L.; Lanvin, J.-D. (2017). Modelling mechanical properties of spruce and Douglas fir timber by means of X-ray and grain angle measurements for strength grading purpose, *European Journal of Wood and Wood Products*, Vol. 75, No. 4, 527–541. doi:10.1007/s00107-016-1149-4
- [40] Burdurlu, E.; Kilic, M.; Ilce, A. C.; Uzunkavak, O. (2007). The effects of ply organization and loading direction on bending strength and modulus of elasticity in laminated veneer lumber (LVL) obtained from beech (*Fagus orientalis* L.) and lombardy poplar (*Populus nigra* L.), *Construction and Building Materials*, Vol. 21, No. 8, 1720–1725. doi:10.1016/j.conbuildmat.2005.05.002
- [41] Han, L.; Han, C.; Dong, L. (2013). Effect of crystallization on microstructure and mechanical properties of poly[(ethylene oxide)-block-(amide-12)]-toughened poly(lactic acid) blend, *Polymer International*, Vol. 62, No. 2, 295–303. doi:10.1002/pi.4300

- [42] Castanié, B.; Peignon, A.; Marc, C.; Eyma, F.; Cantarel, A.; Serra, J.; Curti, R.; Hadji, H.; Denaud, L.; Girardon, S.; Marcon, B. (2024). Wood and plywood as eco-materials for sustainable mobility: A review, *Composite Structures*, Vol. 329, 117790. doi:10.1016/j.compstruct.2023.117790
- [43] Kamke, F. A.; Lee, J. N. (2007). ADHESIVE PENETRATION IN WOOD—A REVIEW, *WOOD AND FIBER SCIENCE*, Vol. 39
- [44] Frihart, C. R. (2012). 9 Wood Adhesion and Adhesives, R. M. Rowell (Ed.), *Handbook of Wood Chemistry and Wood Composites* (0 ed.), CRC Press, 234–271. doi:10.1201/b12487-13
- [45] Ebewe, R. O.; River, B. H.; Koutsky, J. A. (1986). Relationship between phenolic adhesive chemistry and adhesive joint performance: Effect of filler type on fraction energy, *Journal of Applied Polymer Science*, Vol. 31, No. 7, 2275–2302. doi:10.1002/app.1986.070310726
- [46] Siau, J. F. (1984). *Transport Processes in Wood* (Vol. 2), Springer Berlin Heidelberg, Berlin, Heidelberg. doi:10.1007/978-3-642-69213-0
- [47] Marra, A. A. (n.d.). Technology of wood bonding : principles in practice
- [48] Pizzi, A.; Leban, J.-M.; Kanazawa, F.; Properzi, M.; Pichelin, F. (2004). Wood dowel bonding by high-speed rotation welding, *Journal of Adhesion Science and Technology*, Vol. 18, No. 11, 1263–1278. doi:10.1163/1568561041588192
- [49] Niska, K. O. (n.d.). Interactions between wood and synthetic polymers
- [50] Konnerth, J.; Gindl, W. (2006). Mechanical characterisation of wood-adhesive interphase cell walls by nanoindentation, *Holzforschung*, Vol. 60, No. 4, 429–433. doi:10.1515/HF.2006.067
- [51] Kajita, H.; Imamura, Y. (1991). Improvement of physical and biological properties of particleboards by impregnation with phenolic resin, *Wood Science and Technology*, Vol. 26, No. 1. doi:10.1007/BF00225692

## 8. Appendices

**Appendix 1** - ILSS values and fracture surface categorization of the plywood specimens tested under the various combination of pressure and heating times with the three selected adhesives. Rupture mode acronyms are: Co-W: Cohesive Wood; A: Adhesive; A/Co-A: Mixed Adhesive and Cohesive Adhesive; OJ: Out of Joint.

Adh	AHT (min)	P (MPa)	ILSS (MPa)	SD	CoV (%)	Stat group	fracture mode (%)					
							Co-W	Co-A	Mixed			OJ
									A/Co-A	A/Co-A/Co-W	Co-A/Co-W	
<b>Beech</b>												
PLA	5	Vac (0,1)	/	/	/	/	/	/	/	/	/	/
		1	7.48	0.21	2.8	ab	0.0	0.0	<b>85.7</b>	0.0	14.3	0.0
	2	7.52	0.4	5.3	ab	0.0	0.0	<b>100.0</b>	0.0	0.0	0.0	
	15	Vac (0,1)	5.65	0.47	8.4	a	0.0	0.0	<b>100.0</b>	0.0	0.0	0.0
		1	7.66	0.31	4	ab	0.0	0.0	<b>85.7</b>	0.0	14.3	0.0
	2	6.9	0.46	6.6	ab	0.0	0.0	<b>66.7</b>	0.0	33.3	0.0	
rMAPP	5	Vac (0,1)	6.82	2.03	29.7	ab	<b>42.9</b>	0.0	0.0	14.3	0.0	42.9
		1	6.96	1.08	10.4	ab	<b>71.4</b>	0.0	0.0	0.0	14.3	14.3
	2	6.5	1.61	24.7	b	<b>57.1</b>	0.0	0.0	0.0	28.6	14.3	
	15	Vac (0,1)	8.3	0.77	9.2	ab	<b>57.1</b>	0.0	0.0	28.6	0.0	14.3
		1	7.44	1.39	18.7	b	<b>71.4</b>	0.0	0.0	14.3	0.0	14.3
	2	8.08	1.06	13.1	b	<b>100.0</b>	0.0	0.0	0.0	0.0	0.0	0.0
VG	-	1	8.32	1.15	13.8	b	<b>71.4</b>	0.0	0.0	28.6	0.0	0.0
<b>Douglas fir</b>												
PLA	5	Vac (0,1)	2.75	0.42	15.1	ab	42.9	0.0	<b>57.1</b>	0.0	0.0	0.0
		1	3	0.25	8.4	ab	<b>57.1</b>	0.0	0.0	42.9	0.0	0.0
	2	2.98	0.76	25.6	ab	<b>100.0</b>	0.0	0.0	0.0	0.0	0.0	
	15	Vac (0,1)	3.52	0.63	17.9	ab	<b>100.0</b>	0.0	0.0	0.0	0.0	0.0
		1	2.52	0.58	23.1	a	0.0	0.0	16.7	<b>66.7</b>	0.0	16.7
	2	2.27	0.54	23.7	a	<b>50.0</b>	0.0	16.7	33.3	0.0	0.0	
rMAPP	5	Vac (0,1)	3.85	0.98	25.5	ab	<b>85.7</b>	0.0	0.0	14.3	0.0	0.0
		1	4.17	0.97	23.2	ab	<b>66.7</b>	0.0	0.0	0.0	0.0	33.3
	2	4.05	0.73	18	ab	<b>100.0</b>	0.0	0.0	0.0	0.0	0.0	
	15	Vac (0,1)	3.99	0.88	22.1	ab	<b>50.0</b>	0.0	0.0	16.7	0.0	33.3
		1	3.51	1.41	40.2	ab	<b>71.4</b>	0.0	0.0	14.3	0.0	14.3
	2	3.5	1.14	32.7	ab	<b>71.4</b>	0.0	0.0	14.3	0.0	14.3	
VG	-	1	4.44	0.84	18.9	b	<b>57.1</b>	0.0	0.0	14.3	0.0	28.6

**Appendix 2** - ILSS results for plywood interface hybridization with flax fibre for the different wood species and adhesives

Adh	Fibres	ILSS (MPa)	SD	CoV (%)	Main fracture mode(s)
<b>Beech</b>					
rMAPP	No fibres	6.96	1.08	15.5	Co-W (71%)
	Fibres 0°	8.83	0.86	9.7	Co-A (85%)
	Fibres 90°	7.53	0.62	8.2	Co-A (100%)
PLA	No fibres	7.66	0.31	4.0	A/Co-A (85%)
	Fibres 0°	6.76	0.35	5.1	Co-A (100%)
	Fibres 90°	6.57	0.27	4.1	Co-A (100%)
<b>Douglas fir</b>					
rMAPP	No fibres	4.17	0.73	17.5	Co-W (66%)
	Fibres 0°	5.69	1.09	19.1	Co-W (66%)
	Fibres 90°	3.65	0.51	13.9	Co-W (66%)
PLA	No fibres	2.52	0.58	23.1	A/Co-A/Co-W (66%)
	Fibres 0°	3.77	0.51	13.6	A/Co-A/Co-W (43%)   A/Co-A (28%)
	Fibres 90°	3.22	0.49	15.1	Co-W (43%)   Co-A (28%)

**Appendix 3** - ILSS measured for the different wood species, adhesives and with/without fibre reinforcement after the ageing processes

<b>Ag1</b>						<b>Ag2</b>			
Adh	Fibre	ILSS (MPa)	SD	CoV	Main fracture mode(s)	ILSS (MPa)	SD	CoV	Main fracture mode(s)
<b>Beech</b>									
PLA	No	6.48	0.33	5.06	A/Co-A (100%)	9.16	1.28	13.9	A/Co-A/Co-W (62,5%)
	Yes	4.82	0.17	3.55	Co-A (100%)				
PP	No	9.43	0.74	7.82	Co-W (75%)				
	Yes	6.63	0.33	4.99	Co-A (100%)				
<b>Douglas fir</b>									
PLA	No	3.24	0.45	13.9	A/Co-A (50%)   A/Co-A/Co-W (50%)	4.36	0.97	22.2	Co-W (66%)
	Yes	2.82	0.28	10.01	Co-A/Co-W (83%)				
PP	No	4.6	1.85	40.2	Co-W (63%)				
	Yes	5.08	1.29	25.46	A/Co-A/Co-W (50%)   Co-W (37%)				